An innovative digital charge amplifier to reduce hysteresis in piezoelectric actuators

Mohsen Bazghaleh, Steven Grainger, Ben Cazzolato, Tien-fu Lu
School of Mechanical Engineering, The University of Adelaide, SA 5005, AUSTRALIA
Mohsen.bazghaleh@adelaide.edu.au

Abstract

Smart actuators are the key components in a variety of nanopositioning applications, such as scanning probe microscopes and atomic force microscopes. Piezoelectric actuators are the most common actuators among a variety of smart actuators due to their high resolution, low power consumption and wide operating frequency but they suffer hysteresis which affects linearity. In this paper, an innovative digital charge amplifier is presented to reduce hysteresis in stack piezoelectric actuators. Experimental results are presented.

1 Introduction

Piezoelectric actuators have been used in many applications such as atomic force microscopy (Binnig, Quate et al. 1986), inkjet printers (Maeda 1983), fuel injectors in diesel engines (MacLachlan, Elvin et al. 2004), loudspeakers (Kompanek 1965) and many other applications.

The piezoelectric actuator is a type of nanopositioning actuator for which a mechanical displacement results when the electric field across it is changed. Compared to other nanopositioning actuators, typically piezoelectric actuators have high resolution, high force, wide operating frequency and low power consumption.

Creep and hysteresis, which are non-linear characteristics of piezoelectric materials, can reduce the accuracy of a piezoelectric actuator for positioning. When a sudden voltage is applied to a piezoelectric actuator, the length will respond quickly then change slowly due to the creep effect. This is the result of the polarisation of the piezoelectric actuator which continues to change after the applied voltage reaches its final voltage. Commonly the creep effect is an issue at low frequencies (IEEE Standard on Piezoelectricity, 1988).

When the input voltage is gradually increased, the displacement differs from when the voltage is decreased for the same applied voltage which is resulting in hysteresis.

Many techniques have been implemented to reduce the hysteresis such as: model-based control (Goldfarb and Celanovic 1997), displacement feedback control (Fanson and Caughey 1990) and charge control techniques (Fleming and Moheimani 2005).

The Preisach model (Ge and Jouaneh 1995) and the Maxwell resistive model (Goldfarb and Celanovic 1997) are two important mathematical modelling methods. The inverse of these models have been used to remove hysteresis using feedforward elements. There are many drawbacks associated with model-based control techniques. These models are static in nature, as the drive frequency increases the error will also increase. Also they need pre-processing to calculate the appropriate model for each different piezoelectric actuator.

One of the easiest ways to reduce hysteresis is to use the capacitor insertion method (Kaizuka and Siu 1988) which involves using a capacitor in series with the piezoelectric actuator. However this method reduces the operating range of a piezoelectric actuator because of the voltage drop across the capacitor.

Using a charge regulator is another. Comstock (1981) showed that by regulating the charge across the piezoelectric actuator, hysteresis will reduce significantly. The main problem with this approach is that because the sensing capacitor, piezo and opamp are not ideal, the voltage across the sensing capacitor will contain an offset voltage and this can cause drift on the piezoelectric actuator until the output voltage saturates.
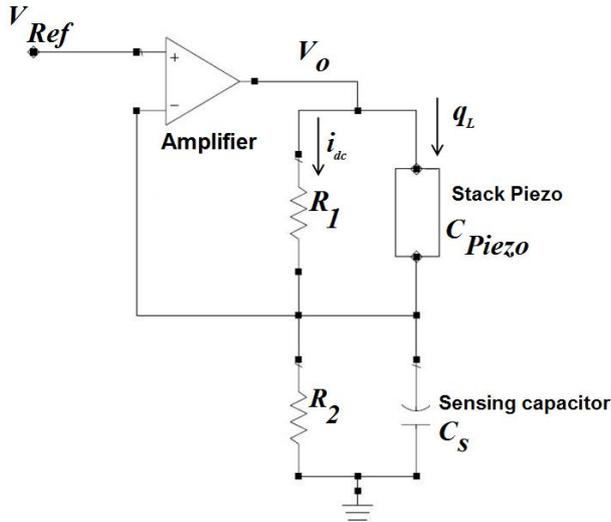
Figure 1: Circuit diagram of analog charge amplifier

Figure 2: Frequency response of a simple analog charge amplifier

Comstok (1981) used an initialization circuit to remove the drift, however, it causes undesirable disturbances at high frequencies. Fleming and Moheimani (2004) proposed an extra voltage feedback loop to improve the low frequency response of their charge amplifier but this extra voltage feedback reduces the bandwidth.

In this paper, a new digital charge amplifier is presented. It significantly reduces the nonlinear behaviour of piezoelectric actuators such as hysteresis. It is more cost effective than analog charge amplifiers and this new design addresses the limited operating frequency of existing piezoelectric actuators. In Section 2 the analog charge amplifier is described. The design and analysis of a digital charge amplifier are presented in Section 3. In Section 4, three different methods to remove the drift are described followed by a conclusion in Section 5.

2 Background

Figure 1 shows a circuit for a simple analog charge amplifier. The feedback loop is used to equalize the reference voltage, V_{ref}, with the voltage across the sensing capacitor. The sensing capacitor is used to integrate the current, and the voltage across it is proportional to charge. R_1 is used to model the opamp input terminal leakage and R_2 is due to the leakage of the sensing capacitor. If the opamp, sensing capacitor and the stack piezo were ideal, R_1 and R_2 will be removed. Therefore, the transfer function will be
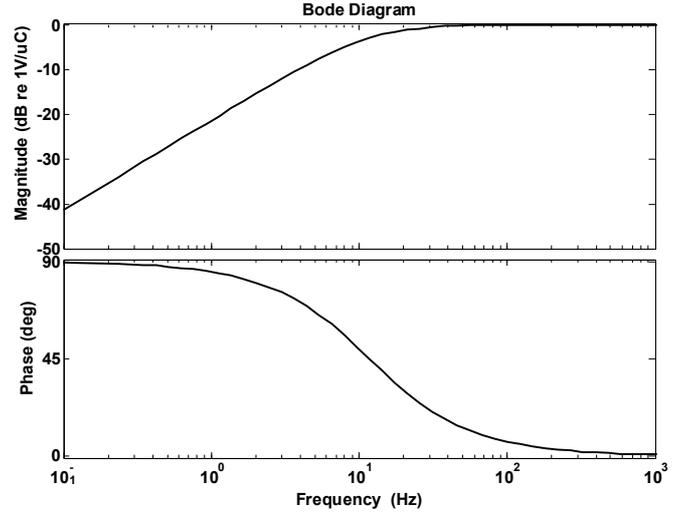
$$\frac{q_L}{V_{ref}} = C_S \tag{1}$$

where C_S is the capacitance of the sensing capacitor. Equation (1) represents an ideal charge amplifier but in practice the main issue is the existence of the two resistors. By considering these resistors the transfer function between stack charge and input voltage will be

$$\frac{q_L}{V_{ref}} = C_S \frac{s}{s + \dfrac{1}{R_1 C_{piezo}}} \tag{2}$$

Equation (2) is a high pass filter with cut off frequency:

$$\omega_c = \frac{1}{R_1 C_{piezo}} \tag{3}$$

At frequencies below ω_C the load impedance is much higher than R_1. Therefore, in contrast with infinite DC impedance, a DC current passes through R_1 which applied DC compliance voltage $V_O = R_1 i_{dc}$ across the piezo (Fleming and Moheimani 2005).

As an example, by using a stack piezo AE0505D44H40 from Nek with a capacitance of $3.4\,\mu F$, and to limit the DC current to $10\,mA$, for the 40V maximum DC offset voltage across the piezo, a parallel resistor $4\,k\Omega$ is needed. As an illustration, figure 2 shows the frequency response of this analog charge amplifier. It can be seen that at frequencies of less than 24 Hz the phase lead exceeds 26 degree which causes distortion for tracking applications.
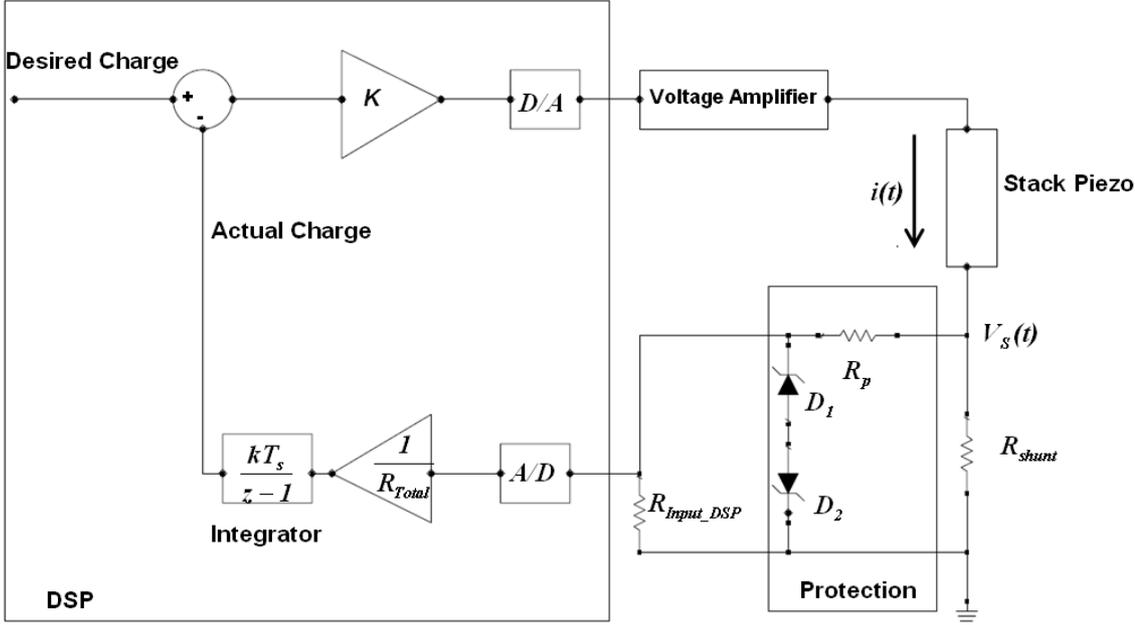
Figure 3: Circuit diagram of a digital charge amplifier

3 Design and analysis

Figure 3 shows the digital charge amplifier that forms the basis of this work. It consists of an analog power amplifier, DAC, ADC and a DSP. A shunt resistor is placed in series with the stack piezoelectric actuator and a protection circuit protects the DSP from high voltage.

In general, this circuit measures the charge across the piezoelectric actuator, and by using a closed-loop control system it tries to equalize the desired input charge signal with the actual charge, q_{Piezo}. To measure the charge, the system integrates the current which passes the piezoelectric actuator and is given by

$$q_{Piezo} = \int i(t)dt \tag{4}$$

Because of protection circuit resistor R_P and the DSP input impedance $R_{InputDSP}$, the piezoelectric actuator current is given by:

$$i(t) = \frac{V_S(t)}{R_{shunt} \parallel \left(R_P + R_{inputDSP}\right)} \tag{5}$$

Substituting Equation (5) into (4) gives the piezo charge:

$$q_{Piezo} = \int \frac{V_S(t)}{R_{shunt} \parallel \left(R_P + R_{inputDSP}\right)} dt \tag{6}$$

The protection resistor and input impedance are in series and together they are in parallel with shunt resistor R_{shunt}, so the total resistance is:

$$R_{Total} = R_{shunt} \parallel \left(R_P + R_{inputDSP}\right) \tag{7}$$

Substituting Equation (7) in (6):

$$q_{Piezo} = \frac{1}{R_{Total}} \int V_S(t)dt \tag{8}$$

Therefore the charge across the piezoelectric actuator is equal to the integral of the voltage across the shunt resistor divided by the total resistance.
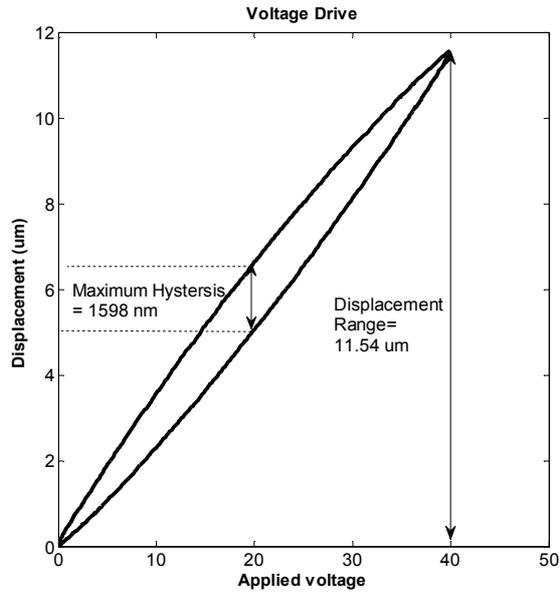
Figure 4: Response of a stack piezoelectric actuator AE0505D44H40 to a 10Hz sine wave driven by a voltage amplifier.

Figures 4 and 5 illustrate the improvement in linearity offered by the new digital charge amplifier compared to a standard voltage amplifier. The displacement of the stack piezoelectric actuator was measured using a strain gauge. For the same displacement range of 11.54 μm, the digital charge amplifier has maximum hysteresis of 144 nm while it is 1598 nm for the voltage amplifier. Therefore the digital charge amplifier has reduced the hysteresis by 91%.

It can be shown that the discrete transfer function from the input (desired charge) to the output (actual charge) is given by $G(z) = \dfrac{z-1}{z-1} = 1$.

In other words, unity gain (up to the Nyquist limit of the A/D rate and loop rate of the controller).

The most significant difficulty in using this technique is drift.

4   Drift removal

Because the analog to digital converter is not ideal, it suffers from current leakage. This can cause a bias voltage V_{bias} in the input. This voltage is the main reason for the drift in charge which is given by:

$$q_{Piezo} = \frac{1}{R_{Total}} \int (V_S(t) + V_{Bias}) dt \qquad (9)$$
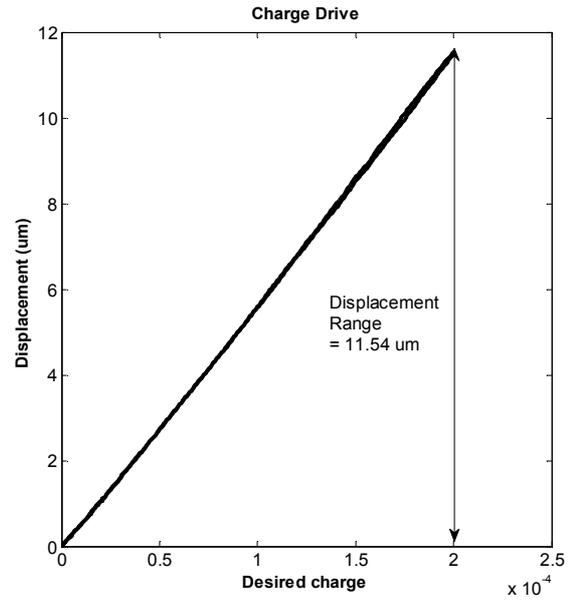

Figure 5: Response of a stack piezoelectric actuator AE0505D44H40 to a 10Hz sine wave with the new digital charge amplifier

This voltage bias can cause miscalculation of the actual charge across the piezoelectric actuator, thus the voltage applied to the piezoelectric actuator will drift and finally saturate.

In the following section, several methods to remove the drift are described.

4.1   Integrator reset

Comstock (1981) uses an analog initialization circuit to reset the circuit to avoid drift. A switch is used to short out the sensing capacitor and sets the voltage across it to zero, thus restarting the circuit periodically.

A similar idea is used in the digital implementation in this paper but here it does not happen periodically. Figure 6 shows the block diagram of this method. Once the voltage across the piezoelectric actuator is equal to zero, the integrator will be restarted. This process is implemented within the DSP so no additional hardware is required.

The result is presented in figure 7. As you can see, this technique distorts the signal when the charge crosses zero.
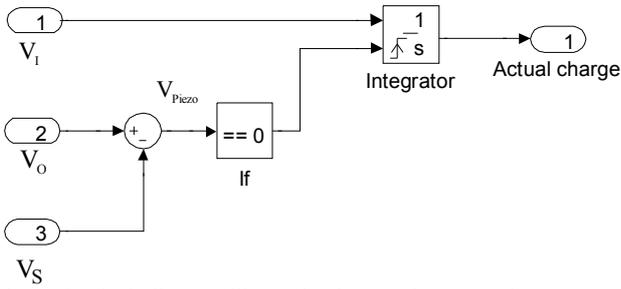
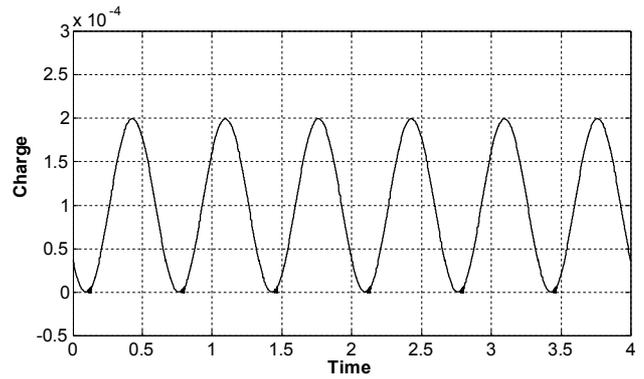Figure 6: Block diagram illustrating how an integrator is reset.
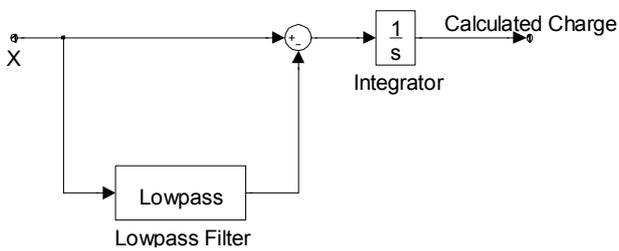

Figure 7 Response of a Integrator reset

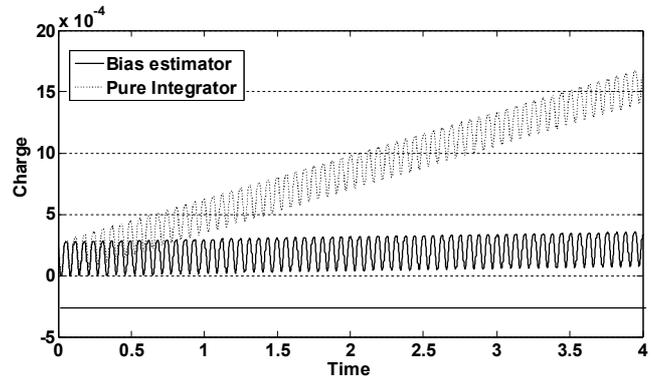Figure 8: Block diagram of a LPF bias estimator

Figure 9: Response of a bias estimator and pure integrator to a 100 rad/sec sine wave with DC offset 10^{-4} C.
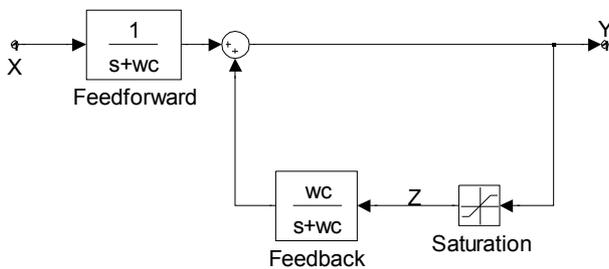

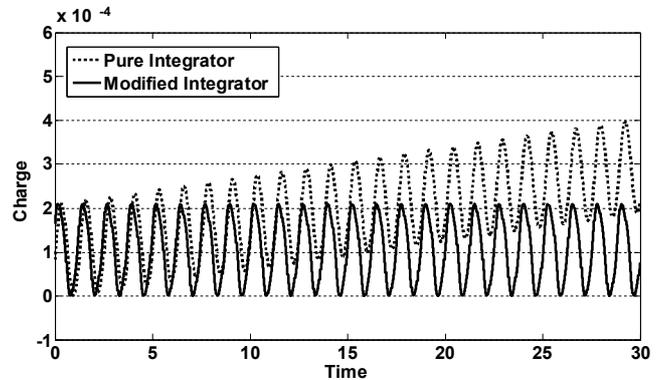Figure 10: Block diagram of a modified integrator

Figure 11: Response of a modified integrator and pure integrator to a 5 rad/sec input sine wave with DC offset 10^{-4} C.

4.2 LPF bias estimator

The easiest way to calculate the bias is using a low pass filter and then removing the bias from the original signal. Figure 8 shows the block diagram of a LPF bias estimator.

The response of a pure integrator and bias estimator to a sine wave of frequency 100 rad/s and a DC bias of 100 μC is shown in Figure 9. It can be seen that the pure integrator has more drift when compared to the bias estimator. After 4 seconds, the pure integrator has 1524 μC error while the bias estimator has 195 μC. This method has reduced the drift by 87%.

4.3 Modified Integrator

A common solution to remove the drift in the output of an integrator is to replace the integrator with a first order low pass filter. However using a LPF can produce errors in the magnitude and phase, especially at frequencies lower than the cut off frequency. To solve this problem a modified integrator can be used (Hu and Wu 1998).

Figure 10 shows the modified integrator. At high frequencies the feedback loop gain is zero. Therefore, the transfer function behaves like a low pass filter. At low frequencies the feedback loop acts to remove the DC drift (Hu and Wu 1998).

If the output signal does not exceed the limitation level in the saturation block, then the transfer function will be a pure integrator. If the input signal reaches the limiting level, the output signal will be

$$\frac{1}{s+w_c}x + \frac{w_c}{s+w_c}z = y \qquad (10)$$

This modified integrator can solve the problem of a pure integrator but the difficulty with this method is to know the limitation of the applied charge.

Figure 11 demonstrates the output of pure integrator and modified integrator shown in Figure 10. It is clear that the pure integrator suffers from drift while the modified integrator has removed the drift.

Although the modified integrator has less drift compared to other drift removal techniques, it has some signal distortion at high frequency. The LPF bias estimator has more drift and it has a simpler implementation. In dynamic applications, if it is known that the signal crosses zero in each period the best option is Integrator reset as it can remove drift completely and distortion is minimal.

5   Conclusion

An innovative digital charge amplifier has been introduced to reduce the non-linear behaviour of a piezoelectric actuator. It reduced the hysteresis by 91% at 10 Hz. Techniques have also been developed to compensate for the drift that plagues charge amplifiers. Compared to analog techniques the digital method shows higher performance and is likely to be far more cost effective.

6   Acknowledgment

References

[Binnig and Quate, 1986] G. Binnig and C. F. Quate. *Atomic Force Microscope*. Physical Review Letters, 56(9): 930-933, 1986.

[Comstock, 1988] R. Comstock. Charge control of piezoelectric actuators to reduce hysteresis effects. *Japan Journal of Applied Physics*, part 2 - Letters, 1981.

[Fanson and Caughey, 1990] J. L. Fanson and T. K. Caughey. Positive position feedback-control for large space structures. *AIAA Journal,* 28(4): 717-724, 1990.

[Fleming and Moheimani, 2004] A. J. Fleming and S. O. R. Moheimani. Hybrid DC accurate charge amplifier for linear piezoelectric positioning. In *Proc. 3rd IFAC Symposium on Mechatronic Systems*, 283–288, 2004.

[Fleming and Moheimani, 2005] A. J. Fleming and S. O. R. Moheimani. A grounded-load charge amplifier for reducing hysteresis in piezoelectric tube scanners. *Review of Scientific Instruments*, 76(7): 73707, 2005.

[Ge and Jouaneh, 1995] P. Ge and M. Jouaneh. Modeling Hysteresis in Piezoceramic Actuators. *Precision Engineering-Journal of the American Society for Precision Engineering*, 17(3): 211-221, 1995.

[Goldfarb and Celanovic, 1997] M. Goldfarb and N. Celanovic. A lumped parameter electromechanical model for describing the nonlinear behavior of piezoelectric actuators. *Journal of Dynamic Systems Measurement and Control-Transactions of the ASME*, 119(3): 478-485, 1997.

[Hu and Wu, 1998] J. Hu and B. Wu. New integration algorithms for estimating motor flux over a wide speed range. *IEEE Transactions on Power Electronics*, 13(5): 969-977, 1998.

IEEE Standard on Piezoelectricity. *ANSI/IEEE standard*, 176-1987, 1988.

[Kaizuka and Siu, 1988] H. Kaizuka and B. Siu. A simple way to reduce hysteresis and creep when using piezoelectric actuators. *Japanese Journal of Applied Physics*, Part 2 (Letters) 27(5): 773-776, 1988.

[Kompanek, 1965] H. W. Kompanek. Loudspeaker with piezoelectric wafer driving elements, Patent No. 3423543, 1965.

[MacLachlan et al., 2004] B. J. MacLachlan and N. Elvin and C. Blaurock and N. J. Keegan. Piezoelectric valve actuator for flexible diesel operation. *Smart Structures and Materials. Industrial and Commercial Applications of Smart Structures Technologies.* E. H. Anderson. Bellingham, SPIE-Int Soc Optical Engineering. 5388: 167-178, 2004.

[Maeda, 1982] J. Maeda. Inkjet printing technologies. *Journal of the Institute of Television Engineers of Japan*, 37(7): 540-545, 1983.

[Newcomb and Flinn, 1982] C. V. Newcomb and I. Flinn. Improving the linearity of piezoelectric ceramic actuators. *Electronics Letters,* 18(11): 442-444, 1982.